Philipp Dancker, Dominik Brunner, Karl Glas, Corinna Dawid and Martina Gastl

Heavy metal adsorption of brewers spent grain in aqueous solution: Impact of mechanochemical esterification

Brewer's spent grain (BSG) has shown promise as a biosorbent to remove heavy metals from water. However, the adsorptive performance of native BSG is limited and modifications to enhance said performance suffer from extensive use of organic solvents. A potential solution is mechanochemical esterification, in which solid-phase reactivity is enhanced through high-energy milling. In this study, the adsorptive performance of BSG, which has been mechanochemically esterified with citric acid, was investigated (BSGE). The maximum adsorption capacities q_{max} for nickel Ni(II), cadmium Cd(II), and lead Pb(II) ions were evaluated following bottle-point isotherm procedure in a buffered solution of sodium acetate, with a pH value of 4.5. The impact of the heavy metal initial concentration C_0 1 – 250 mg/L on the equilibrium capacity q_e was studied and the data was fitted to the Langmuir and Freundlich models. The Langmuir model was best to describe data variance, as such q_{max} was used to describe adsorptive performance: 65.83 mg/g for Pb(II), 24.72 mg/g for Cd(II), and 15.11 mg/g for Ni(II), with Langmuir constants K_L of 0.149 L/mg, 0.031 L/mg and 0.023 L/mg, respectively. These findings indicate that mechanochemical esterification yielded a 232.2 % Pb(II), 576.3 % Ni(II) and 164.4 % Cd(II) gain in adsorptive performance over native BSG. Based on molar comparisons, adsorptive affinities were determined as follows: BSGE (Pb > Ni ≈ Cd) and BSG (Pb > Cd > Ni).

Descriptors: BSG, spent grain, biosorbent, brewing, heavy metals, water remediation, adsorption, mechanochemistry

1 Introduction

Through human industrial activities soluble heavy metal ions are introduced into surface water, soils, and rivers. They persist and accumulate through biomagnification in plants and animals as they do not decompose unlike organic pollutants. If not removed they migrate into the human food chain where they harm the consumer [1]. A subgroup of toxic heavy metals is composed of the soluble ions cadmium Cd, nickel Ni, and lead Pb. Despite their toxicity, they are ubiquitously used and subsequently the most common toxic metals in wastewater [2]. Anthropogenic sources for those three toxic metals are numerous. From mining, metal alloys, batteries, solar-cells, over paints, plastics, plumbing, water pipes, soldering, and electroplating, resulting in their widespread distribution. If incorporated by humans they are carcinogenic, neurodegenerative, and affect systemically [3]. For this reason, the maximum legal concentrations in drinking water are set by various organisations around the world. The World Health Organization (WHO) in their Guidelines for drinking-water quality, the European Union (EU) in the DIRECTIVE (EU) 2020/2184, the United Kingdom (UK) in the Water Supply (Water Quality) Regulations, and Germany in the Ordinance on the Quality of Water Intended for Human Consumption. Currently, all four set the limit for lead in drinking water to 10 µg/L with a reduction in the future. For nickel the EU, the UK, and Germany allow 20 µg/L, while the WHO allows 70 µg/L. For cadmium the WHO and Germany allow 3 µg/L, while the EU and the UK allow up to 5 µg/L. A variety of methods with their specific advantages and disadvantages for water remediation exist to reduce heavy metal containing effluent into the environment or to develop new sources for drinking water. There are chemical precipitation [4], coagulation and flocculation [5], ion exchange [6], electrochemical removal [7], reverse osmosis [8, 9], and adsorption [10]. Chemical precipitation works by exceeding the solubility product of the contamination and filter out the precipitate. While being feasible and inexpensive it produces the filtrate as a toxic sludge and is ineffective for trace level contamination [11]. Coagulation and flocculation methods are used to remove turbidity and total suspended solids but remove heavy metals as well if they are adsorbed to the aggregated suspended particles. It shares the same disadvantages as the chemical precipitation method. During ion exchange charged contaminations are removed through acidic or alkaline functional groups on the material. With controlled modification of the ion exchange resin the removal process can be made more or less selective for a specific contamination. To regenerate the resin, a strong opposing acid or base is required to displace the contaminants from the resin, resulting in waste water highly concentrated with the removed contaminants. A further downside of the ion exchange method

https://doi.org/10.23763/BrSc25-06dancker

Authors

Philipp Dancker (ORCID ID: 0009-0002-6455-7409), Martina Gastl (ORCID ID: 0000-0002-6485-6727), Research Center Weihenstephan for Brewing and Food Quality, Technical University of Munich, Freising, Germany; Dominik Brunner (ORCID ID: 0009-0001-7851-4373), Corinna Dawid (ORCID ID: 0000-0001-5342-2600), Technical University of Munich, Chair of Food Chemistry and Molecular Sensory Science, Professorship for Functional Phytometabolomics Germany; Karl Glas (ORCID ID: 0009-0004-3498-3663), Technical University of Munich, Chair of Food Chemistry and Molecular Sensory Science, Freising, Germany, Technical University of Munich, Professorship of Functional Materials for Food Packaging, Freising, Germany; corresponding authors: philipp.dancker@tum.de, dominik.brunner@tum.de

is the cost of ion exchange resin. The electrochemical removal of heavy metals works without chemicals but has high running and purchase costs for the equipment and power supply. Furthermore, the electrodes are susceptible for unwanted side reaction which reduce their lifetime, demand maintenance, and have so far impeded widespread use. Almost all solutes, including salts, heavy metals, and microorganisms can be removed with reverse osmosis through a semi-permeable membrane by applying an external pressure to overcome the natural osmotic pressure. Chemicals are needed to postpone fouling and scaling of the membrane and maintain a stable flux as well as high energy cost to operate the pumps to maintain the transmembrane pressure. The contaminants are concentrated in the retentate and depending on the specific permeability of a heavy metal, trace level amounts cannot be removed [12]. Adsorption methods are based on intermolecular force between the solute and the adsorbents surface. Depending on the bonding mechanism it can be highly specific and reduce even trace amounts of a contaminant. It is easy to implement in either a slurry reactor or a fixed-bed filter. However, the ecological and economic benefits of adsorption are highly dependent on the adsorbent´s source material and production thereof. That is why there has been a spiked interest in the development of adsorbents from agro-industrial residues and lignocellulose (LC) in particular [13]. Adsorptive performance of native LC is typically considered to be low [14, 15], thus research has been focussed on chemical modifications to enhance said performance [16]. A major hurdle of this approach has been the low solubility of LC in common solvents, therefore most research utilizes extraction of cellulose and organic solvents to facilitate enhanced modification [17, 18]. This approach has led to the development of great modifications strategies, but causes a shift in application, away from the low-cost and ecologically friendly field of operation LC was originally intended for. Potential solutions to this problem are modifications using mechanochemical activation, in which solid-phase reactivity is enhanced through mechanical energy. Recently [19], BSG was mechanochemically esterified with citric acid (BSGE) to increase adsorptive performance of methylene blue by 537.2 %. BSG is a highly abundant biomass with an output 0.8 Mt in the UK, 1.8 Mt in Germany, 12.4 Mt in Amerika, 11.9 Mt in Asia, and 3.1 Mt in Afrika in 2022 [20]. Due to its microbial susceptible and short storage life it is in need for a further utilisation method. While the most common method up to date is the use as feed for ruminants, there are many other utilisation methods for BSG [21].

This study´s aim is to characterize the adsorptive performance of BSGE and BSG towards Pb(II), Ni(II), and Cd(II), using bottle-point isotherm studies. The impact of the heavy metal initial concentration C_0 on the equilibrium capacity is studied and Langmuir and Freundlich models are assessed for their suitability to describe the data variance.

2 Materials and methods

2.1 Chemicals

Acetic acid (Ac), sodium acetate (NaOAc) anhydrous, sodium hydroxide (NaOH), and lead(II) nitrate ($Pb(NO_3)_2$) from Merck KGaA (Darmstadt, Germany). Hydrochloric acid (HCl), 30 wt. %, and nitric acid (HNO_3), 69 wt. %, from VWR International GmbH (Ismaning, Germany). Nickel(II) nitrate ($Ni(NO_3)_2$) hexahydrate and cadmium(II) nitrate ($Cd(NO_3)_2$) tetrahydrate from Sigma Aldrich (Steinheim, Germany). Citric acid (CA) from Carl Roth GmbH (Karlsruhe, Germany). All bought chemicals are of analytical grade or of higher purity. Ultrapure water was produced on site with a Berrytec® miniUPUV+ (Harthausen, Germany) with a maximum conductivity of 0.05 µS/cm, or minimum resistivity of 20 MΩcm respectively.

2.2 BSG preparation

BSG samples were obtained from the Staatsbrauerei Weihenstephan (Freising, Germany) and drawn from one batch of the Original Helles production line. Hot water extraction was performed at 80 °C for 30 min at a mass to volume ratio of 1 g per 10 L water. Subsequently, solid-liquid separation was performed using a decanter centrifuge at pilot scale (Flottweg SE, Vilsbiburg, Germany). Samples were then dried at 80 °C to constant mass (48 h). Esterification with citric acid was conducted by means of mechanical activation using a custom ball-mill setup. In brief, samples (20 g) and citric acid (8 g) were placed in a preheated reaction vessel (7.6 L) containing grinding balls with a diameter of 6.35 mm and a stirrer element. Volumetric ratios of citric acid to BSG $Ø_{CA/BSG}$, BSG to grinding balls $Ø_{BSG/B}$ and grinding balls to total vessel volume $Ø_{B/V}$ are given as follows: 0.27, 0.2 and 0.04. Mechanically activated esterification was facilitated through convective heating (140 °C) for 30 min and simultaneous, high-energy ball-milling (400 rpm). For a detailed description of this experimental setup, refer to [19]. Mechanically activated, esterified BSG was labelled as BSGE. Additionally, BSG samples were treated as described above, but without the addition of the esterification agent and labelled BSG. This was done to provide a baseline of adsorptive performance and elucidate on the impact of esterification on Pb(II), Cd(II), and Ni(II) adsorption, whilst normalizing the potential impact of particle size reduction on adsorptive performance.

2.3 Adsorption experiments

Adsorption trials were conducted as bottle-point isotherm studies. Hence, adsorbent mass (BSG, BSGE) was held constant at 100 mg per volume of 50 mL and the impact of the adsorbate (Pb(II), Cd(II), Ni(II)) initial concentration C_0 (1, 2, 5, 10 ,15, 20, 25, 30, 40, 50, 75, 100, 150, 200, 250 mg/L) on the equilibrium concentrations C_e and the equilibrium capacities q_e were studied, respectively. For all isotherms, stock, and working solution, a 40 mM sodium acetate buffer solution with a pH value of 4.5 was used with a weigh-in of 1543 mg Ac and 1171 mg NaOAc per litre of ultrapure water. The pH value of 4.5 is necessary to prevent the precipitation of Cd, Pb, or Ni as insoluble salts at the concentrations used. A final adjustment of the pH value was done using negligible quantities of 1 M HCl and 1 M NaOH. A stock solution of each metal separately with a concentration of 1 g/L of Ni(II), Cd(II), and Pb(II), was prepared. From this stock solution the initial concentrations C_0 for the adsorption isotherm were prepared in 50 mL buffered solution inside in a test tube made from PE plastics on 100 ± 5 mg BSG. After shaking with 150 rpm for 42 h the suspensions were centrifuged at 4000 g for 10 min and an aliquot of the supernatant was taken to measure the equilibrium concentration C_e. Each sample for ICP-MS was preserved with 1 % HNO_3 until measurement. q_e was calculated

using the general mass balance equation (Equation 1), where V is the liquid phase volume (L) and m is the adsorbent mass (g). Subsequently, the data was fitted to the Langmuir (Equation 2) and Freundlich (Equation 3) models, where q_{max} is the maximum capacity (mg/g), K_L is the Langmuir constant (L/mg), $K_F\,(\frac{mg}{g}\,(\frac{L}{mg})^{1/n_F})$ and n_f (–) are the Freundlich constant and heterogeneity factor. Model fits were performed with nonlinear regression using Origin Pro from OriginLab (Northampton, Massachusetts, USA).

$$q_e = (C_o - C_e)\frac{V}{m} \quad \text{(Eq. 1)}$$

$$q_e = q_{max}\frac{K_L C_e}{1 + K_L C_e} \quad \text{(Eq. 2)}$$

$$q_e = K_f C_e^{\frac{1}{n_f}} \quad \text{(Eq. 3)}$$

2.4 Cation measurements

The metal ion content was determined from the supernatant of the batch experiments after centrifugation to determine C_e using an ICP-MS (NexION 2000 ICP Mass Spectrometer, PerkinElmer LAS GmbH, Rodgau, Germany) according to DIN EN ISO 17294-2 [22]. The samples were transferred with a peristaltic pump through PTFE tubes and nebulized inside a high sensitivity SilQ cyclonic spray chamber. All elements were measured using a kinetic energy discrimination (KED) mode using a flow of 4.8 mL/min 99.999 % pure helium to reduce polyatomic interferences. The system was tuned according to the manufacturer's specifications to minimize oxides and double charged ions. For a list of other system parameters, refer to the supporting information.

2.5 Anion measurements

The anion content was determined from the supernatant of the batch experiments without HNO_3 preservation after centrifugation to determine a change of the nitrate content which would indicate a multilayer adsorption process. An IC-CD (Dionex Integrion HPIC, Thermo Fisher Scientific GmbH, Dreieich, Germany) according to DIN EN ISO 10304-1 [23] was used.

2.6 Elemental and molecular composition

The elemental composition of BSG was done according to DIN EN 17053 [24] after a microwave assisted digestion in HNO_3 according to DIN EN 13805 [25] and FDA Elemental Analysis Manual for Food and Related Products [26]. 750 ± 10 mg of BSG were mixed with 7.5 mL HNO_3 and 7.5 mL ultrapure water inside a closed PTFE tube (CEM GmbH, Kamp-Lintfort, Germany). The mixture was heated to 160 °C and kept at this temperature for 30 min for a complete digestion of the organic matrix. The cellulose, hemicellulose, and lignin content of the BSG was determined according to the handbook of agricultural testing and research methodology III chapter 6.5.2 as neutral detergent fibre, acid detergent fibre, and acid detergent lignin. Ash, raw fibre, and raw ash were determined according to commission regulation (EC) No 152/2009 [27].

3 Results and discussion

3.1 Chemical characterization

Adsorption is a process of physico-chemical interaction between the solute and the adsorbent. This interaction can be in the form of ion exchange, surface complexation and precipitation, hydrogen bonds, or electrostatic interactions [28]. The BSG was obtained from a Bavarian pale lager beer with 100 % barley malt (Staatsbrauerei Weihenstephan, Freising, Germany). All three examined metals Cd, Ni, and Pb were below the limit of quantitation (LOQ) with 0.04 mg/kg BSG dry weight. Elements above the LOQ were phosphorus P with 3272 mg/kg, nitrogen N with 41600 mg/kg, silicon Si with 241 mg/kg, potassium K with 15.6 mg/kg, calcium Ca with 39.5 mg/kg, magnesium Mg with 29.5 mg/kg, and zinc Zn with 2.9 mg/kg. From these only phosphorus and nitrogen are present in quantities that could influence adsorption. Phosphorus is bound as phosphates in terrestrial plants [29] and most of it as phytic acid in barley grain [30]. Other forms of phosphor occur in sugar phosphates, ATP, nucleic acids, and phospholipids, which are partially hydrolysed by phytase enzymes during malting [31]. In the brewing process the soluble fraction of phosphates is extracted into the beer and the remaining is discharged and left in the BSG. Calculating with a standard atomic weight of 30.97 g/mol for phosphor and assuming all of it as phosphates, that would equal an amount of 10.57 µmol of phosphate per isotherm data point (100 mg BSG). Following [32] that amount of phosphate has the potential to adsorb the same amount of divalent metal ions like Cd(II), Ni(II), and Pb(II).

$$R - O - PO_3H_2 + M^{2+} \leftrightarrow R - O - PO_3M + 2H^+ \quad \text{(Eq. 4)}$$

With standard atomic weights of 112.41 g/mol for Cd, 58.69 g/mol for Ni, and 207.2 g/mol for Pb, the proportion of q_{max} for BSG just with its phosphate content could potentially be 11.9 mg/g for Cd, 6.2 mg/g for Ni, and 21.9 mg/g for Pb, respectively. The reaction between phytate and divalent metal ions to form insoluble salts is known in brewing and leads to a drop in the pH value during mashing [23].

The nitrogen content of BSG represents the protein fraction of barley which was not extracted into the wort. After several washing steps before using the BSG as a biosorbent the amount of free amino acids is negligible, and only structural protein is left. 41600 mg/kg nitrogen with a conversion factor of 6.79 equals a protein content of 28.25 %(w/w), which makes BSG a sought-after food supplement for ruminants. The average composition of BSG protein´s free functional amino (NH_2), amide ($CONH_2$), carboxyl (COOH), and hydroxyl (O–H) groups was theoretically estimated using literature data [33], a table of which is presented in the supporting information. The COOH has the highest potential to adsorb divalent metal ions through a mechanism of ion exchange and complexation analogue to the binding mechanism in weak cation exchange resins. Since two COOH groups are needed to adsorb one divalent metal ion the amount of 42.06 µmol could potentially adsorb a maximum of 21.03 µmol, which would equal 23.6 mg/g for Cd, 12.3 mg/g for Ni, and 43.6 mg/g for Pb, respectively.

BSG LC content was 71.6 % (w/w), consisting of 28.5 % cellulose, 50 % hemicellulose and 21.5 % lignin. Relative to other LC sources,

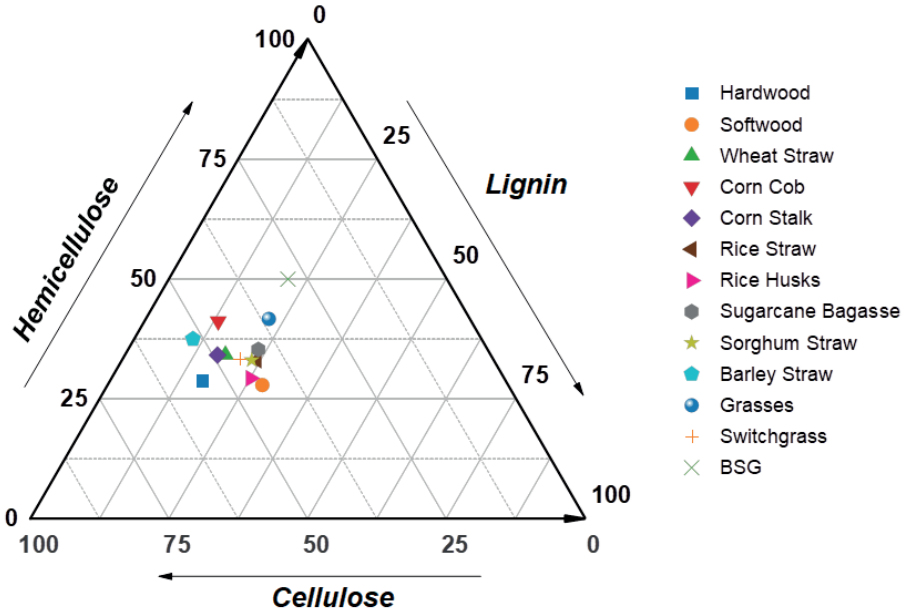

Fig. 1 **BSG LC composition against literature data [34], adapted to a ternary compositional diagram**

BSG LC is of lower cellulose and lignin contents, which is shown in figure 1 as a ternary compositional diagram [34]. Due to analytical limitations of LC, in conjunction with polymer heterogeneity, no theoretical composition of LC functionalities can be postulated. Therefore, the hypothesized, adsorption capacities of native BSG phosphates and proteins represent theoretical upper limits of those fractions. Correlations between the theoretical limits and observed adsorptive behaviour of BSG cannot be postulated due to unknown a) surface to total mass fraction and b) composition of LC functionalities.

ATR-FTIR analysis was used for qualitative assessment of changes in surface chemistry before and after adsorption of the respective metal species onto BSGE (Fig. 2). FTIR spectra were post-processed using moving-average polynomial regression and b-spline interpolation. Bands at 1726 1/cm and 1167 1/cm correspond to carbonyl C=O and C-O stretching of ester and carboxyl groups [17, 35–37]. The absence of a pronounced peak at 1726 1/cm and shift towards 1730 1/cm indicates the involvement of the C=O group in the adsorption of Pb(II), Ni(II), and Cd(II). Additionally, C-O associated peaks at 1167 1/cm did shift to 1160 1/cm, indicating involvement of these functionalities as well. With regards to the involvement of hydroxyl groups -OH, a shift in the broad peak from 3406 1/cm to 3337 1/cm would indicate the involvement of these functionalities in the adsorption process. However, although BSGE loaded with the respective metals displayed peaks at 3406 1/cm, BSGE did not show a pronounced peak before adsorption, thus no conclusions on the involvement of hydroxyl groups can be drawn.

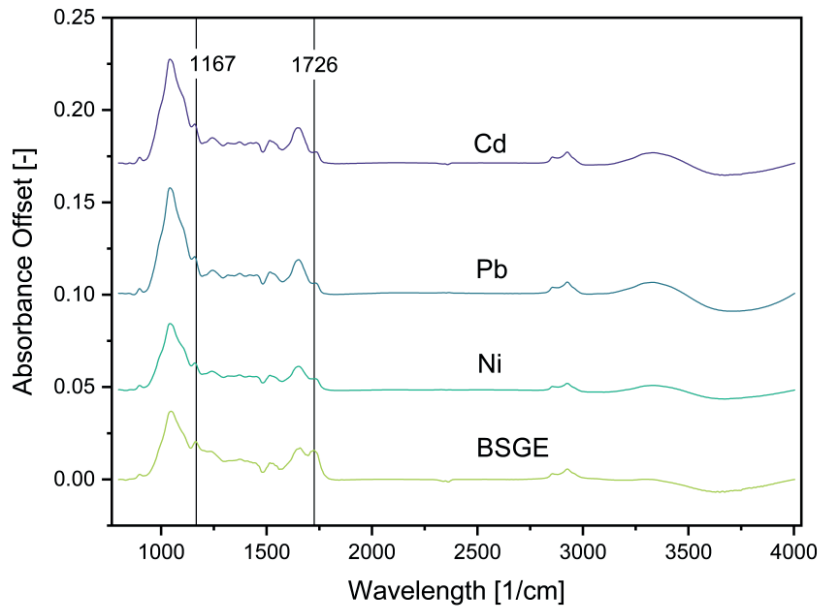

Fig. 2 **Baseline corrected FTIR spectra stack plot of: BSGE before and after the adsorption of the respective metal species (Ni, Pb, Cd). Band at 1726 1/cm: C=O, 1167 1/cm C-O**

3.2 Buffer selection

The overall premise of the buffer selection studies was to ensure pH stability within and between the bottle-point isotherm trials of a given adsorbent/adsorbate pair. This was done to provide a foundation of comparability between metal species and their respective affinity towards BSG and BSGE, as well as assessment of relative gain in adsorptive performance due to esterification. A common way of handling the influencing factor pH as an experimental parameter, is to adjust the initial pH_0 through the addition of an acid or base [38–41]. To evaluate this approach for the adsorbent/adsorbate pairs presented within this work, singular bottle-point studies of Pb(II), Ni(II), and Cd(II) (C_0 250 mg/L) were set to an initial pH_0 4.5 and pH stability was measured after the adsorbent/adsorbate pairs reached equilibrium (42 h), the data of which is shown in table 2. Initial pH_0 4.5 was chosen based on solubility product and redox potential considerations of the respective metal salts in solution. As shown, pH deviated between 1.8 % (BSG, 250 mg/L Pb(II)) and 27.8 % (BSGE, 250 mg/L Pb(II)). The average decrease in pH was highest among esterified BSG samples, which is assumed to be associated with deprotonation of carboxylic functionalities. Subsequently, pH stability trials were conducted with Pb(II), to study the effects of BSG type, pH_0, and Pb(II) concentration C_{Pb} on the pH: BSG and BSGE (100 mg) were dispersed in 50 mL

Table 2 pH stability of adsorbent (BSG/BSGE) and adsorbate (Pb, Ni, Cd) pairs

	pH
pH_0	4.50
BSGE Pb	3.25
BSGE Cd	3.62
BSGE Ni	3.61
BSG Pb	4.42
BSG Cd	4.99
BSG Ni	5.53

Table 3 Summary of Langmuir model parameters of Pb, Ni and Cd onto BSG and BSGE

	K_L (L/mg)	q_{max} (mg/g)	q_{max} (mmol/g)
BSGE Pb	0.149	65.83	0.318
BSGE Cd	0.031	24.72	0.220
BSGE Ni	0.023	15.11	0.257
BSG Pb	0.211	28.23	0.136
BSG Cd	0.008	15.04	0.134
BSG Ni	0.044	2.62	0.045

aqueous solution of different pH_0 (4; 5; 6) and pH was measured after 5 min. Then, different volumes (50-3000 µL) of Pb(II) stock solution (10 g/L) were added to facilitate Pb(II) concentration jumps within the range used for adsorption trials and pH was measured, which is shown in figures 3 a, b and c.

It is apparent, that the evolution of BSGE pH is a function of C_{Pb} and widely independent of pH_0. The development of pH BSG however, is influenced by both factors, C_{Pb}, and pH_0. Although pH_0 was sufficient for the construction of isotherms in other research, it was concluded that, for the adsorbent/adsorbate pairs within this work, pH instability would introduce a variable error to the isotherm studies and data comparability would consequently suffer. Therefore, buffering with 40 mM sodium acetate and acetic acid at pH 4.5 was chosen. Buffering introduces a constant error by means of competitive adsorption, as such buffer concentration was minimized. At 40 mM the change of the pH value was less than 0.03 which is the maximum allowed measurement deviation for a calibration standard in the DIN EN ISO 10523 [42].

3.3 Adsorption experiments

In total, three metals (Pb(II), Ni(II), and Cd(II)) were evaluated for their ability to adsorb onto brewer´s spent grain, that has been esterified with citric acid through mechanical activation in a custom ball-mill (BSGE) and brewer´s spent grain, which has been milled without the addition of an esterification agent (BSG). All data points were obtained using the standard bottle-point isotherm procedure. As such, equilibrium capacities q_e and equilibrium concentrations C_e were studied as a function of different initial concentrations C_0 (1 – 250 mg/L), whilst adsorbent mass was held constant at 100 mg.

Figure 4 a depicts the adsorption of Pb(II) onto BSG and BSGE. BSG showed Langmuir-type behaviour and was thus fitted to the Langmuir model at R^2 97.2 %. Regression of the Freundlich model did not converge onto the BSG data. Langmuir model parameters were estimated at q_{max} 28.2 mg/g and K_L 0.21 L/mg. Regression of BSGE did converge at R^2 99.2 %. However, a good visual fit was only obtained in the initial, near linear part of the curve and model regression did under evaluate the data point C_0 250 mg/L by 5.9 %, thus the extrapolated q_{max} 65.8 mg/g could be prone to undervaluation. The Freundlich model was only able to explain R^2 95.8 % of the data´s variance and did not show good convergence for a majority of data points. K_F was estimated at 12.6 ($\frac{mg}{g}(\frac{L}{mg})^{1/n_F}$) and n_f was 2.68. Based on comparative assessment of q_{max}, esterification of BSG lead to an 233.2 % increase in adsorptive performance of Pb(II).

Figure 4 b shows the adsorption of Ni(II) onto BSG and BSGE. The Langmuir model was able to describe 99.5 % of the variance of BSG and q_{max} was estimated within the boundaries of interpolation at 1.8 mg/g. Adsorption data of Ni(II) onto BSGE was prone to more uncertainty than the other isotherms with standard deviations of up to 9.4 %. The Langmuir model was able to describe 95.9 % of the data´s variance and showed good visual convergence, although under evaluation of the C_0 250 mg/L data point was observed. Thus, the estimated q_{max} 15.1 mg/g is prone to extrapolation errors. The Freundlich model showed better convergence of R^2 98.1 % (K_F 1.2 ($\frac{mg}{g}(\frac{L}{mg})^{1/n_F}$) n_f 2.2), which could be an indicator of either multilayer adsorption, or adsorption onto a heterogenous surface. However,

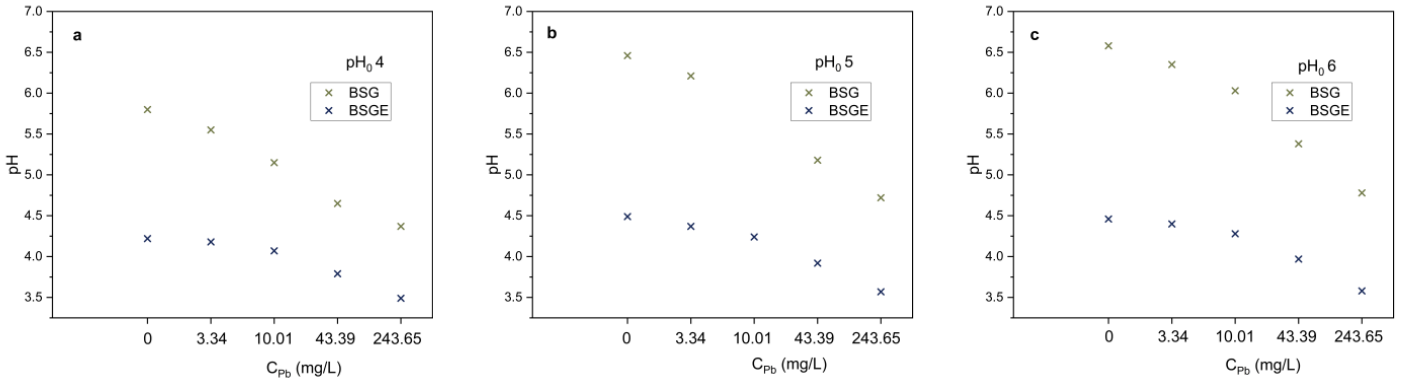

Fig. 3 a to c: pH stability studies. Effect of C_{Pb} and initial pH_0 on the pH for BSG and BSGE, respectively

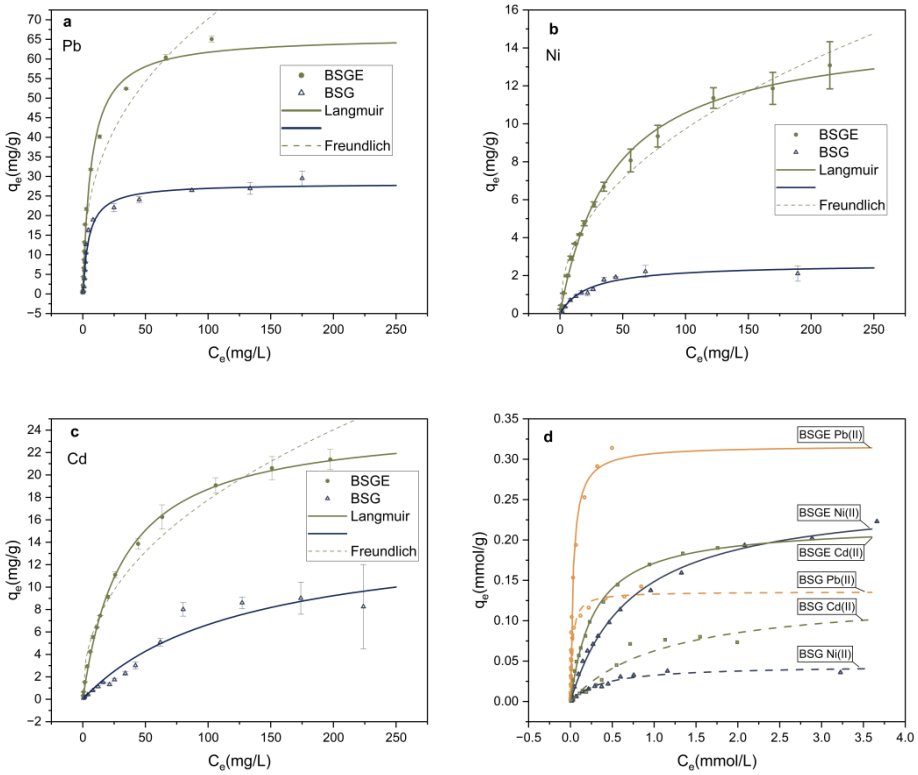

Fig. 4 **a to c: Adsorption isotherms of a) Pb(II), b) Ni(II), and c) Cd(II) onto BSG and BSGE, respectively. Data variance explained by Langmuir (lines) and Freundlich models (dashed lines). Figure 4 d: molar comparison isotherm plot of Pb(II) (circles, yellow), Ni(II) (triangles, blue), and Cd(II) (squares, green) onto BSGE and BSG**

both the Langmuir and the Freundlich model represent empirically adopted versions of mechanistic equations, thus derivation of adsorption mechanisms based on bottle-point isotherm data is limited. To evaluate the possibility of multilayer adsorption, nitrate equilibrium concentrations were quantified (refer to the supplementary information for nitrate quantification data). Nitrate did not partake in the adsorption process. Multilayer adsorption typically necessitates the alternating adsorption of cations and anions, thus it was concluded that no multilayer adsorption did take place. Therefore, it is more likely, that Ni(II) adsorption onto BSGE follows Langmuir-type behaviour. Based on the relative increase of q_{max}, esterification of BSG was able to increase Ni(II) adsorption by 576.3 %.

Figure 4 c shows the adsorption isotherms of Cd(II) onto BSG and BSGE. The Langmuir model was able to explain 93.4 % of the variance introduced through the adsorption of BSG. However, the rate change of adsorption per unit-step in equilibrium concentration was observed to be low within the pseudo-linear part of the Langmuir function, indicating low affinity of Cd(II) towards BSG. Additionally, data uncertainty was inconsistent and increased with higher C_e values (max. deviation 45.6 %) averaging out at 9.4 %. The maximum adsorption capacity of Cd(II) onto BSG was estimated at 15.0 mg/g. Convergence of the Langmuir model for the Cd(II) adsorption onto BSGE, was able to explain 99.8 % of the data´s variance and estimated q_{max} at 24.7 mg/g. The Freundlich model was only able to explain 97.2 % of the variance and significantly over evaluated the slope at the end of the adsorption-data spectrum. Based on the relative increase in q_{max}, esterification of brewer´s spent grain was able to increase the adsorptive performance by 164.4 %.

Figure 4 d shows the molar comparison plot of Pb(II), Ni(II), and Cd(II) adsorption onto BSGE and BSG, respectively. Regression of the Langmuir model, estimated the molar maximum adsorption capacities of BSGE and BSG q_{max}, as follows. BSGE: Pb 0.318 mmol/g, Ni 0.257 mmol/g and Cd 0.220 mmol/g. BSG: Pb 0.136 mmol/g, Ni 0.045 mmol/g and Cd 0.134 mmol/g. Based on comparative assessment of molar q_{max} values, an affinity series of Pb(II), Ni(II) and Cd(II) towards the functional groups of native BSG was postulated: Pb > Cd > Ni. After mechanochemical esterification and taking data uncertainty into consideration, a shift in the affinity series was observed: Pb > Ni ≈ Cd. Esterification of BSG introduces carboxylic functionalities (-COOH) to the material's active adsorption sites. Thus, the relative increase in adsorptive performance of the respective metal species can be attributed to BSG´s gain in COOH functional groups. Ni(II) exhibited the highest, relative gain in q_{max} (576.25 %), followed by Pb(II) (233.18 %) and Cd(II) (164.36 %), indicating different affinities of Pb(II), Ni(II) and Cd(II) towards carboxylic functionalities: Ni > Pb > Cd, which is in accordance with the affinity shift introduced through esterification. Interestingly, Ni and Cd express similar affinities towards esterified BSG only at the higher end of the equilibrium concentration spectrum and deviate at the pseudo-linear part of the Langmuir model. This is mainly attributed to differences in K_L (Ni: 0.023 L/mg, Cd: 0.031 L/mg). Due to the mechanistic limitations of adsorption isotherm model parameters in liquid phase adsorption and data uncertainty, reasons for this observation cannot be hypothesized [43]. In practical applications however, Cd may express higher affinity towards BSGE, as these are typically operated at the lower end of the equilibrium concentration spectrum.

4 Conclusion

Clean drinking water is one of the most important aspects for human life and the production of food and beverages. The ever-expanding industrialization discharges toxic heavy metals into the water cycle, endangering it. A subgroup of those heavy metals consists of Pb, Cd, and Ni, which are characterized by their high toxicity combined with extensive technical applications, amplifying their harmful potential. Adsorption is an easy-to-implement process to remove metal ions or other contaminants from water either in a fixed-bed adsorber or a slurry reactor which can be integrated in a water treatment plant. Within this work, adsorption of Pb(II), Ni(II) and Cd(II) onto mechanochemically esterified, brewer´s spent grain (BSGE) was characterized using bottle-point isotherm procedure. The Langmuir model was best to describe data variance, as such the maximum equilibrium capacity q_{max} was used to asses adsorptive performance: 65.83 mg/g for Pb(II), 24.72 mg/g for Cd(II), and 15.11

mg/g for Ni(II). Thus, mechanochemical esterification was able to increase q_{max} by 232.2 % for Pb(II), 576.3 % for Ni(II) and 164.4 % for Cd(II), against native BSG. Affinity of heavy metals towards BSGE was highest for Pb(II), followed by Ni(II) and Cd(II) (Pb > Ni ≈ Cd). Affinities towards BSG were determined to be (Pb > Cd > Ni). Although Ni(II) showed the highest gain in q_{max}, Cd(II) may still adsorb better onto BSGE in practical applications due to a higher K_L, which impacts the slope of the isotherm at lower equilibrium concentrations. In conclusion, BSG and BSGE were successfully evaluated for their potential in the adsorptive removal of Pb(II), Ni(II) and Cd(II) from aqueous solution. Both materials were able to adsorb the respective heavy metal species and mechanochemical esterification led to a significant increase in adsorptive performance. These findings indicate that BSGE could be a promising biosorbent for industrial process water treatment. Further studies should emphasize the comparative assessment of biosorbents and modifications thereof, to provide the groundworks for techno-economical evaluation of potential biosorbents.

Declaration of competing interest

The authors declare that they have no known competing financial interests or personal relationships that could have appeared to influence the work reported in this paper.

Author contributions

Philipp Dancker and Dominik Brunner both contributed equally to this work.

5 References

1. Vardhan, K. H.; Kumar, P. S. and Panda, R. C.: A review on heavy metal pollution, toxicity and remedial measures: Current trends and future perspectives, Journal of Molecular Liquids, **290** (2019), p. 111197.
2. Zhou, Q.; Yang, N.; Li, Y.; Ren, B.; Ding, X.; Bian, H. et al.: Total concentrations and sources of heavy metal pollution in global river and lake water bodies from 1972 to 2017, Global Ecology and Conservation, **22** (2020), e00925.
3. Zamora-Ledezma, C.; Negrete-Bolagay, D.; Figueroa, F.; Zamora-Ledezma, E.; Ni, M.; Alexis, F. et al.: Heavy metal water pollution: A fresh look about hazards, novel and conventional remediation methods, Environmental Technology & Innovation, **22** (2021), p. 101504.
4. Chen, Q.; Yao, Y.; Li, X.; Lu, J.; Zhou, J. and Huang, Z.: Comparison of heavy metal removals from aqueous solutions by chemical precipitation and characteristics of precipitates, Journal of Water Process Engineering, **26** (2018), pp. 289-300.
5. Shrestha, R.; Ban, S.; Devkota, S.; Sharma, S.; Joshi, R.; Tiwari, A. P. et al.: Technological trends in heavy metals removal from industrial wastewater: A review, Journal of Environmental Chemical Engineering, **9** (2021), no. 4, p. 105688.
6. Saleh, T. A.; Mustaqeem, M. and Khaled, M.: Water treatment technologies in removing heavy metal ions from wastewater: A review, Environmental Nanotechnology, Monitoring & Management, **17** (2022), p. 100617.
7. Tran, T.-K.; Chiu, K.-F.; Lin, C.-Y. and Leu, H.-J.: Electrochemical treatment of wastewater: Selectivity of the heavy metals removal process, International Journal of Hydrogen Energy, **42** (2017), no. 45, pp. 27741-27748.
8. Hoek, E. M. V.; Weigand, T. M. and Edalat, A.: Reverse osmosis membrane biofouling: causes, consequences and countermeasures, npj Clean Water, **5** (2022), no. 1.
9. Oesinghaus, H.; Wanken, D.; Lupp, K.; Gastl, M.; Elsner, M. and Glas, K.: Incipient Biofouling Detection via Fiber Optical Sensing and Image Analysis in Reverse Osmosis Processes, Membranes, **13** (2023), no. 6.
10. Chai, W. S.; Cheun, J. Y.; Kumar, P. S.; Mubashir, M.; Majeed, Z.; Banat, F. et al.: A review on conventional and novel materials towards heavy metal adsorption in wastewater treatment application, Journal of Cleaner Production, **296** (2021), p. 126589.
11. Lewis, A.: Precipitation of Heavy Metals, in Rene, E. R.; Sahinkaya, E.; Lewis, A. and Lens, P. N. (Eds.): Sustainable Heavy Metal Remediation, Springer International Publishing, Cham, 2017, pp. 101-120.
12. Kapepula, V. L. and Luis, P.: Removal of heavy metals from wastewater using reverse osmosis, Frontiers in Chemical Engineering, **6** (2024).
13. Quadros Melo, D. de; Oliveira Sousa Neto, V. de; Freitas Barros, F. C. de; Raulino, G. S. C.; Vidal, C. B. and do Nascimento, R. F.: Chemical modifications of lignocellulosic materials and their application for removal of cations and anions from aqueous solutions, Journal of Applied Polymer Science, **133** (2016), no. 15.
14. Li, Q.; Chai, L. and Qin, W.: Cadmium(II) adsorption on esterified spent grain: Equilibrium modeling and possible mechanisms, Chemical Engineering Journal, **197** (2012), pp. 173-180.
15. Du, Z.; Zheng, T.; Wang, P.; Hao, L. and Wang, Y.: Fast microwave-assisted preparation of a low-cost and recyclable carboxyl modified lignocellulose-biomass jute fiber for enhanced heavy metal removal from water, Bioresource technology, **201** (2016), pp. 41-49.
16. Wan Ngah, W. S. and Hanafiah, M. A. K. M.: Removal of heavy metal ions from wastewater by chemically modified plant wastes as adsorbents: a review, Bioresource technology, **99** (2008), no. 10, pp. 3935-3948.
17. Li, Q.; Chai, L.; Wang, Q.; Yang, Z.; Yan, H. and Wang, Y.: Fast esterification of spent grain for enhanced heavy metal ions adsorption, Bioresource technology, **101** (2010), no. 10, pp. 3796-3799.
18. Hokkanen, S.; Bhatnagar, A. and Sillanpää, M.: A review on modification methods to cellulose-based adsorbents to improve adsorption capacity, Water research, 91 (2016), pp. 156-173.
19. Brunner, D.; Dancker, P.; Gastl, M.; Dawid, C. and Glas, K.: Adsorptive removal of methylene blue by mechanochemically esterified brewer´s spent grain, ACS Sustainable Resource Management (2025 (Submitted but not yet accepted)).
20. Barth, S. J. and Meier H.: BarthHaas report hops 2021/2022 (2022).
21. Emmanuel, J. K.; Nganyira, P. D. and Shao, G. N.: Evaluating the potential applications of brewers' spent grain in biogas generation, food and biotechnology industry: A review, Heliyon, **8** (2022), no. 10, e11140.
22. DIN EN ISO 17294-2:2017-01, Wasserbeschaffenheit_- Anwendung der induktiv gekoppelten Plasma-Massenspektrometrie (ICP-MS)_- Teil_2: Bestimmung von ausgewählten Elementen einschließlich Uran-Isotope (ISO_17294-2:2016); Deutsche Fassung EN_ISO_17294-2:2016, Beuth Verlag GmbH, Berlin.
23. DIN EN ISO 10304-1:2009-07, Wasserbeschaffenheit_- Bestimmung von gelösten Anionen mittels Flüssigkeits-Ionenchromatographie_- Teil_1: Bestimmung von Bromid, Chlorid, Fluorid, Nitrat,

Nitrit, Phosphat und Sulfat (ISO_10304-1:2007); Deutsche Fassung EN_ISO_10304-1:2009, DIN Media GmbH, Berlin.
24. DIN EN 17053:2018-03, Futtermittel_- Probenahme- und Untersuchungsverfahren_- Bestimmung von Spurenelementen, Schwermetallen und anderen Elementen in Futtermitteln mittels ICP-MS (Multimethode); Deutsche Fassung EN_17053:2018, DIN Media GmbH, Berlin.
25. DIN EN 13805:2014-12, Lebensmittel_- Bestimmung von Elementspuren_- Druckaufschluss; Deutsche Fassung EN_13805:2014, DIN Media GmbH, Berlin.
26. U.S. Food & Drug Administration: Elemental Analysis Manual (EAM) for Food and Related Products: EAM, 2020.
27. European Union: Commission Regulation (EC) No 152/2009 of 27 January 2009 laying down the methods of sampling and analysis for the official control of feed (Text with EEA relevance): Document 32009R0152, 2009.
28. Gadd, G. M.: Biosorption: critical review of scientific rationale, environmental importance and significance for pollution treatment, Journal of Chemical Technology & Biotechnology, **84** (2009), no. 1, pp. 13-28.
29. White, P. J. and Hammond, J. P.: Phosphorus nutrition of terrestrial plants, in Kok, L. J. de; Hawkesford, M. J.; Stulen, I.; White, P. J. and Hammond, J. P. (Eds.): The Ecophysiology of Plant-Phosphorus Interactions, Springer Netherlands, Dordrecht, 2008, pp. 51-81.
30. Ockenden, I.; Dorsch, J. A.; Reid, M.; Lin, L.; Grant, L. K.; Raboy, V. et al.: Characterization of the storage of phosphorus, inositol phosphate and cations in grain tissues of four barley (Hordeum vulgare L.) low phytic acid genotypes, Plant Science, **167** (2004), no. 5, pp. 1131-1142.
31. Briggs, D. E.: Malts and malting, 1. ed., Blackie Academic & Professional, London, 1998.
32. Wang, R. and Guo, S.: Phytic acid and its interactions: Contributions to protein functionality, food processing, and safety, Comprehensive reviews in food science and food safety, **20** (2021), no. 2, pp. 2081-2105.
33. Waters, D. M.; Jacob, F.; Titze, J.; Arendt, E. K. and Zannini, E.: Fibre, protein and mineral fortification of wheat bread through milled and fermented brewer's spent grain enrichment, European Food Research and Technology, **235** (2012), no. 5, pp. 767-778.
34. Cai, J.; He, Y.; Yu, X.; Banks, S. W.; Yang, Y.; Zhang, X. et al.: Review of physicochemical properties and analytical characterization of lignocellulosic biomass, Renewable and Sustainable Energy Reviews, **76** (2017), pp. 309-322.
35. Gan, T.; Zhang, Y.; Su, Y.; Hu, H.; Huang, A.; Huang, Z. et al.: Esterification of bagasse cellulose with metal salts as efficient catalyst in mechanical activation-assisted solid phase reaction system, Cellulose, **24** (2017), no. 12, pp. 5371-5387.
36. Hoang, M. T.; Pham, T. D.; Pham, T. T.; Nguyen, M. K.; Nu, D. T. T.; Nguyen, T. H. et al.: Esterification of sugarcane bagasse by citric acid for Pb2+ adsorption: effect of different chemical pretreatment methods, Environmental science and pollution research international, **28** (2021), no. 10, pp. 11869-11881.
37. Widsten, P.; Dooley, N.; Parr, R.; Capricho, J. and Suckling, I.: Citric acid crosslinking of paper products for improved high-humidity performance, Carbohydrate Polymers, **101** (2014), pp. 998-1004.
38. Zhu, H.-X.; Cao, X.-J.; He, Y.-C.; Kong, Q.-P.; He, H. and Wang, J.: Removal of Cu^{2+} from aqueous solutions by the novel modified bagasse pulp cellulose: Kinetics, isotherm and mechanism, Carbohydrate Polymers, **129** (2015), pp. 115-126.
39. Zhou, C.-G.; Gao, Q.; Wang, S.; Gong, Y.-S.; Xia, K.-S.; Han, B. et al.: Remarkable performance of magnetized chitosan-decorated lignocellulose fiber towards biosorptive removal of acidic azo colorant from aqueous environment, Reactive and Functional Polymers, **100** (2016), pp. 97-106.
40. Zheng, L.; Peng, D. and Meng, P.: Promotion effects of nitrogenous and oxygenic functional groups on cadmium (II) removal by carboxylated corn stalk, Journal of Cleaner Production, **201** (2018), pp. 609-623.
41. Fan, S.; Zhou, J.; Zhang, Y.; Feng, Z.; Hu, H.; Huang, Z. et al.: Preparation of sugarcane bagasse succinate/alginate porous gel beads via a self-assembly strategy: Improving the structural stability and adsorption efficiency for heavy metal ions, Bioresource technology, **306** (2020), p. 123128.
42. DIN EN ISO 10523:2012-04, Wasserbeschaffenheit_- Bestimmung des pH-Werts (ISO_10523:2008); Deutsche Fassung EN_ISO_10523:2012, DIN Media GmbH, Berlin.
43. Mudhoo, A. and Pittman, C. U.: Adsorption data modeling and analysis under scrutiny: A clarion call to redress recently found troubling flaws, Chemical Engineering Research and Design, **192** (2023), pp. 371-388.

Received 7 March 2025, accepted 15 April 2025